# Supporting Information

## Enriched Oxygen Vacancies in $SnO_{2-x}$ with Narrow Bandgap for Highly Sensitive Gas Sensing

Pei-Xuan Wu,[abc] Bo-Jing Ruan,[b] Ke-Feng Li,[abc] Wei-Hua Deng,*[a] Yong-Jun Chen,*[b] and Gang Xu[b]

[a]*College of Chemistry and Materials Science, Fujian Normal University, Fuzhou, Fujian, 350007, P. R. China.*
[b]*State Key Laboratory of Structural Chemistry, and Fujian Provincial Key Laboratory of Materials and Techniques toward Hydrogen Energy, Fujian Institute of Research on the Structure of Matter, Chinese Academy of Sciences, Fuzhou, Fujian 350002, P. R. China.*
[c]*Fujian College, University of Chinese Academy of Sciences, Fuzhou, Fujian 350002, P. R. China.*

Corresponding author: W-H. Deng (*E-mail: dengweihua@fjnu.edu.cn*), and Y-J. Chen (*E-mail: chenyongjun@fjirsm.ac.cn*)

# Experimentation

## Characterization

Powder X-ray diffraction (PXRD) of samples were recorded on a Rigaku Smartlab MiniFlex 600 X-ray diffractometer using Cu *Kα* radiation ($\lambda$ = 1.54178 Å) at 30 kV and 15 mA. The pdf card of $SnO_2$ was derived from the Jade software. Scanning electron microscope (SEMZEISS-300) was operated at 3.0 kV. Transmission electron microscope (TEM) images were obtained on a JEOL-2010 transmission electron microscope at an acceleration voltage of 200 kV. X-ray photoelectron spectroscopy (XPS) data was collected on a Thermo Scientific ESCALAB 250 Xi XPS system. UV-visible absorption curve and transmittance data were collected on a Perkin–Elmer Lambda 950 spectrophotometer using $BaSO_4$ as a white standard, use the powder synthesized in the same bottom with $SnO_{2-x}$ thin film.

## Synthesis of $SnO_{2-x}$.

Glass substrates (1 × 3 cm) were cut and sequentially ultrasonically cleaned in ethanol and deionized water, followed by drying for later use. A solution (Solution A) was prepared by dissolving 357 mg KBr in 10 mL deionized water. Separately, 350.6 mg $SnCl_4·5H_2O$ was dissolved in 60 mL glacial acetic acid to form Solution B. The two solutions were mixed thoroughly, followed by the addition of 10 mL anhydrous ethanol, and the mixture was ultrasonicated for 5 min. The resulting precursor solution was divided into ten 8 mL Teflon-lined autoclaves, with 0.0237 g (0.2 mmol) Sn powder added to each. Cleaned glass substrates were immersed in the solutions, leaning against the inner walls of the vessels. The autoclaves were sealed and heated at 200 °C for 12 h in an oven. Upon completion, $SnO_{2-x}$ thin films were uniformly deposited on the substrates, with $SnO_{2-x}$ powder samples also collected from the reaction mixture.

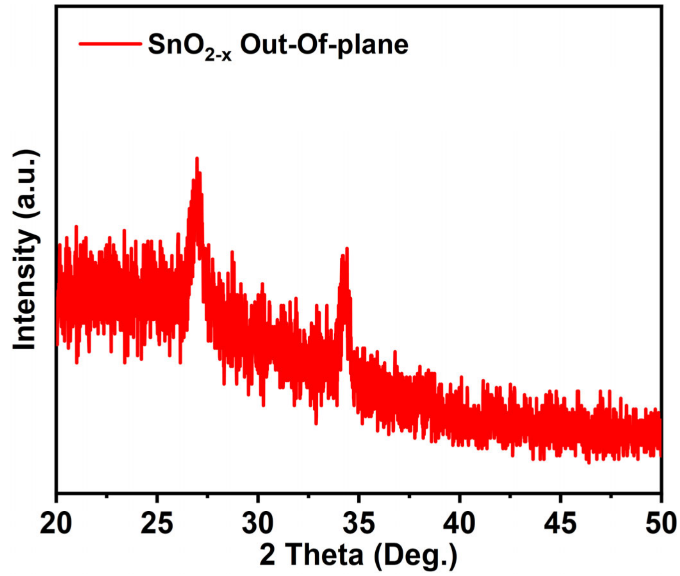


Fig. S1 Out-of-plane XRD pattern of $SnO_{2-x}$.

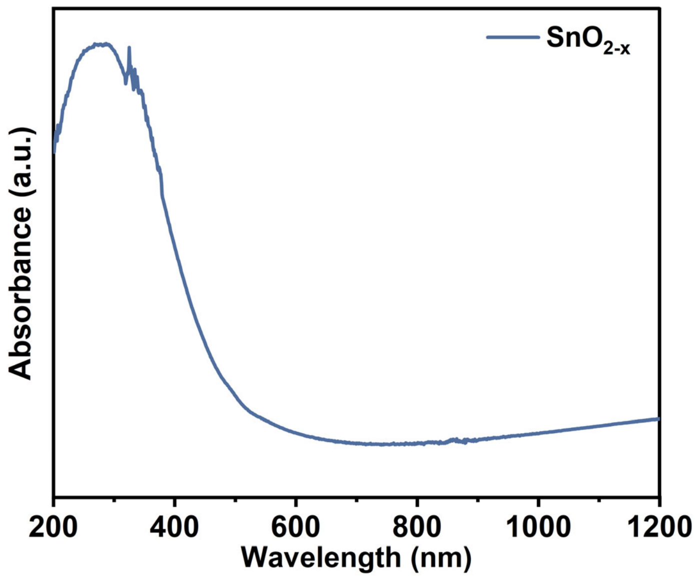


Fig. S2 Solid-state ultraviolet absorption spectroscopy of $SnO_{2-x}$.

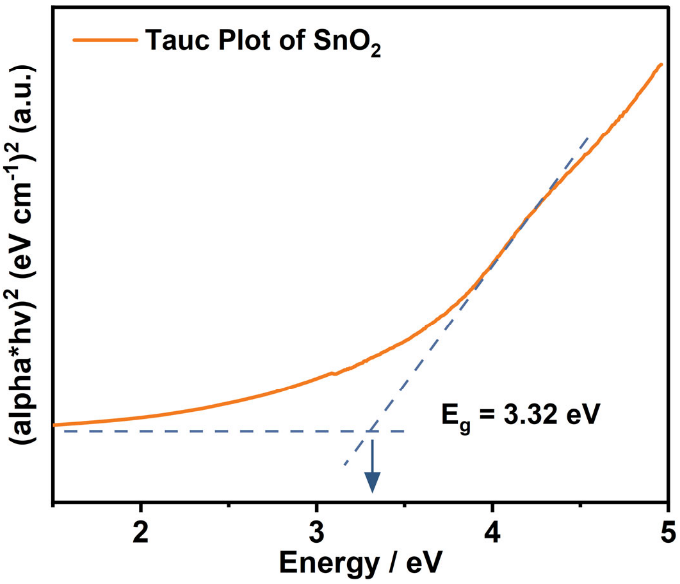

Fig. S3 Tauc plot of $SnO_2$.

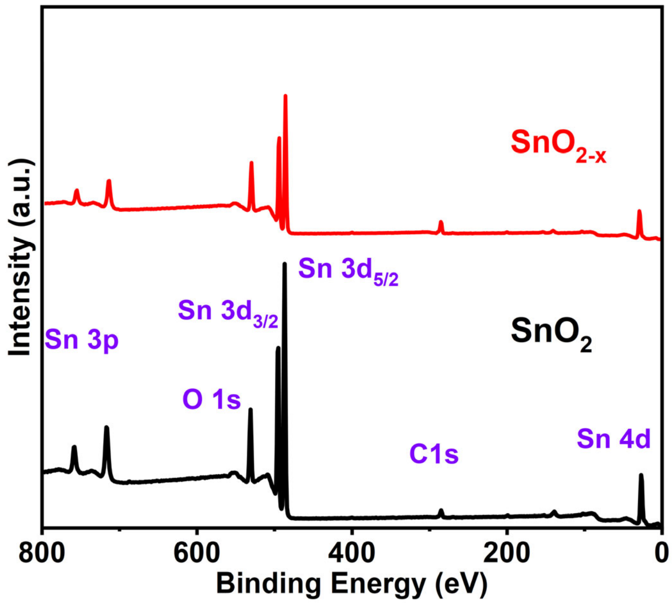

Fig. S4 XPS general spectrum of $SnO_2$ and $SnO_{2-x}$.

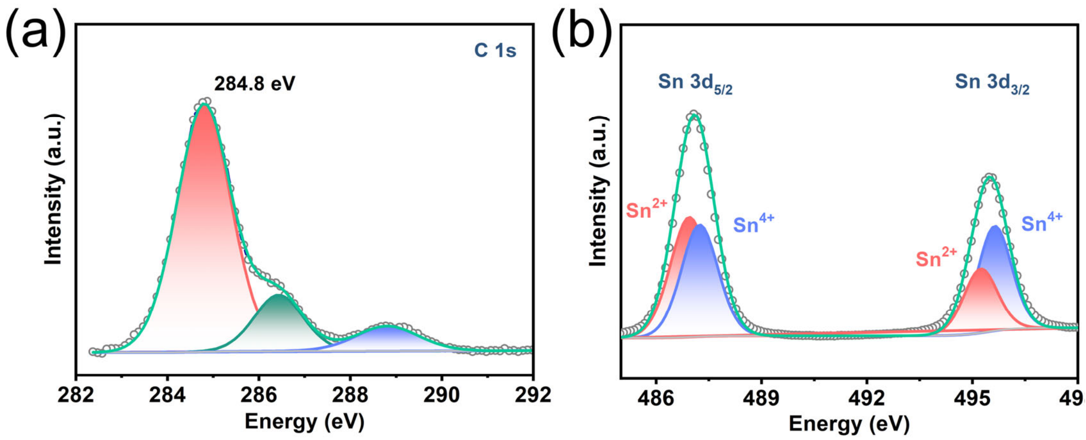


Fig. S5 XPS spectrum of C 1s and Sn 3d ($3d_{5/2}$ and $3d_{3/2}$) of $SnO_{2-x}$.

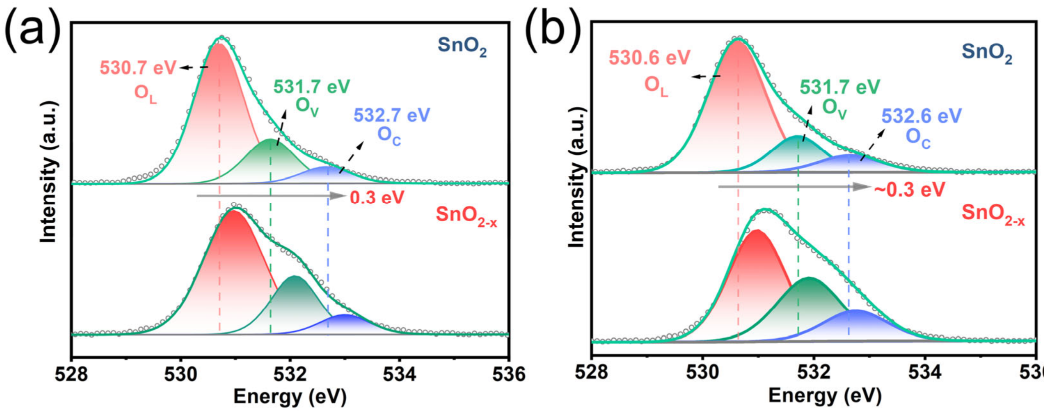


Fig. S6 XPS spectrum of O 1s for multiple sample comparisons.

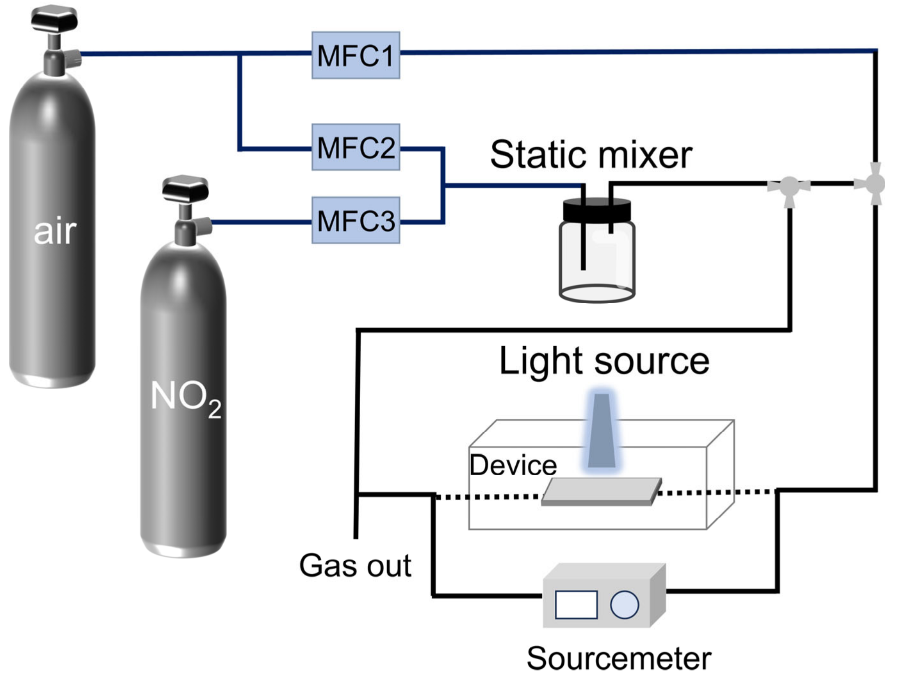


Fig. S7 Gas sensing system.

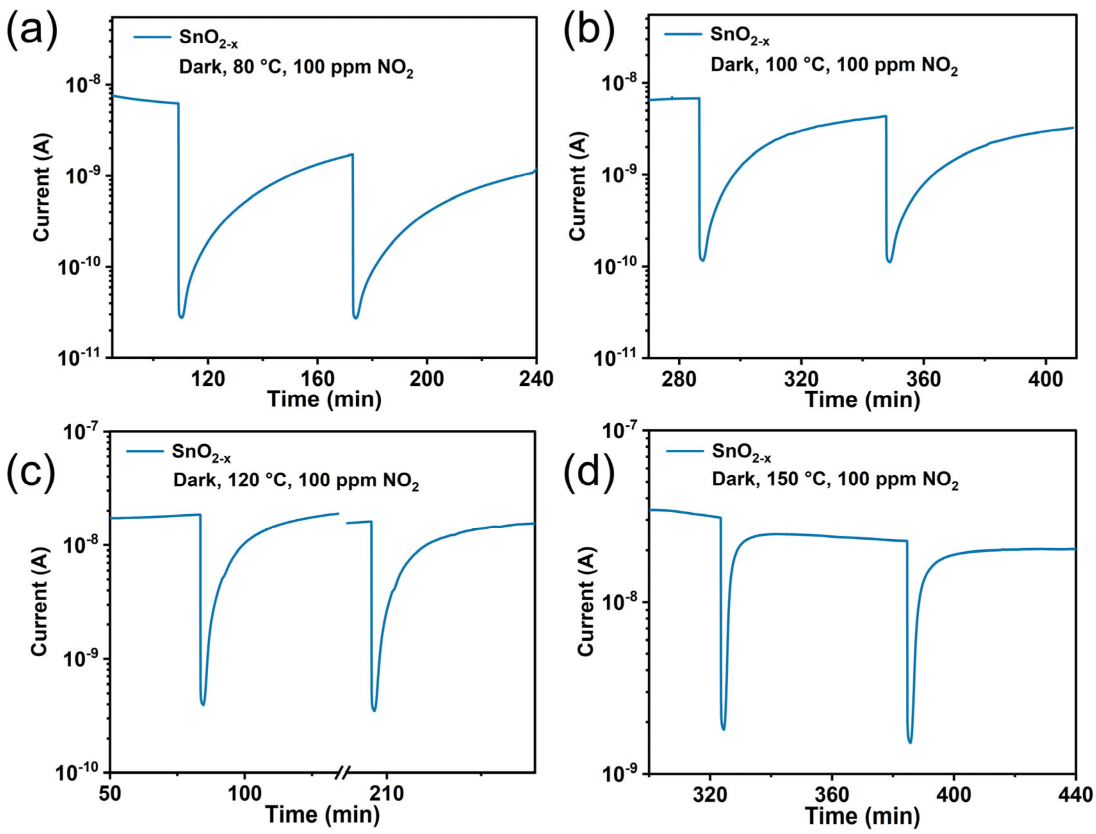


Fig. S8 Response curves to $NO_2$ under different temperatures.

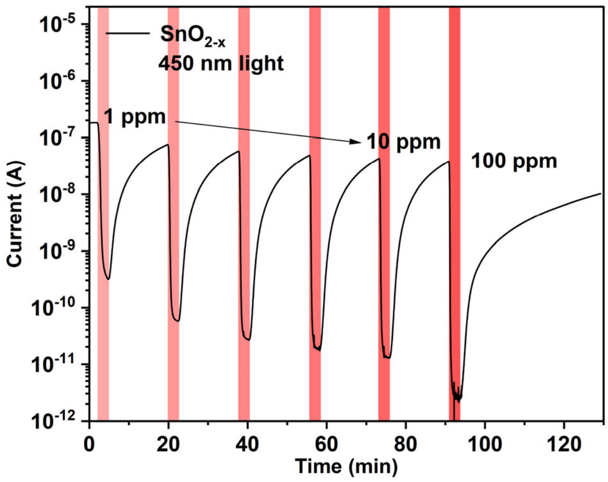


Fig. S9 Response-recovery curve with concentration of 1 - 100 ppm.

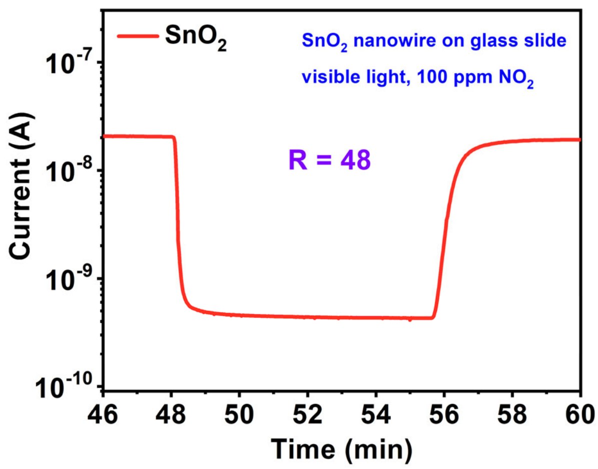


Fig. S10 Response of $SnO_2$ to 100 ppm $NO_2$ under visible light.

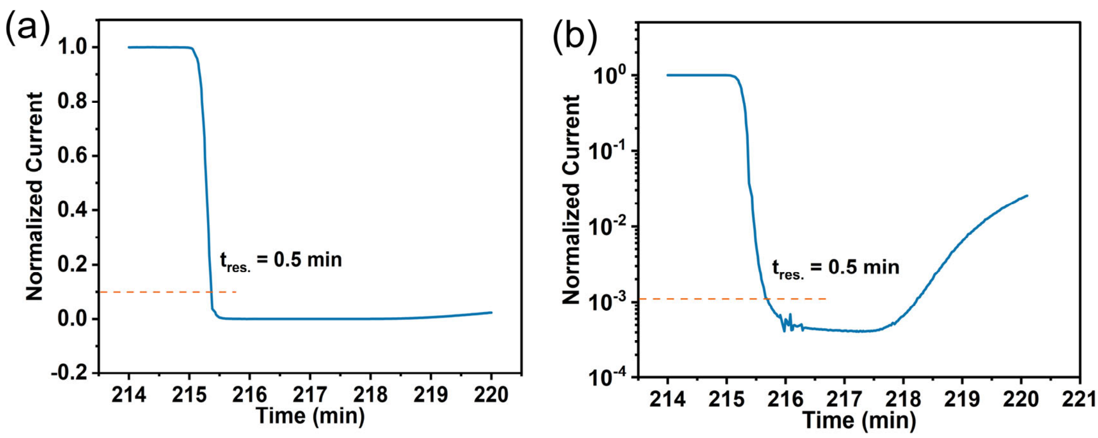


Fig. S11 Schematic of steady state on response to 10 ppm $NO_2$.

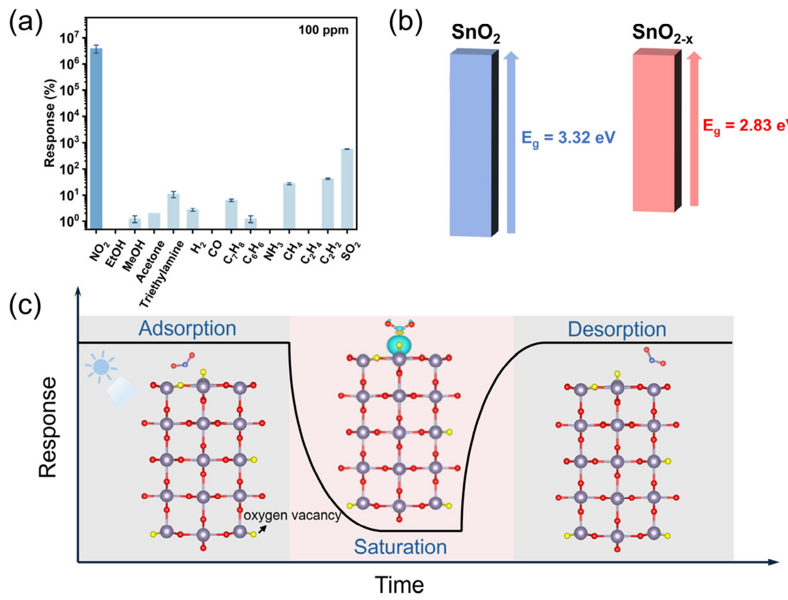


Fig. S12 (a) Responses comparison among $NO_2$ and interference gases of $SnO_{2-x}$. (b) Energy level between $SnO_2$ and $SnO_{2-x}$. (c) Conceptual diagram of mechanism of $SnO_{2-x}$ to $NO_2$.

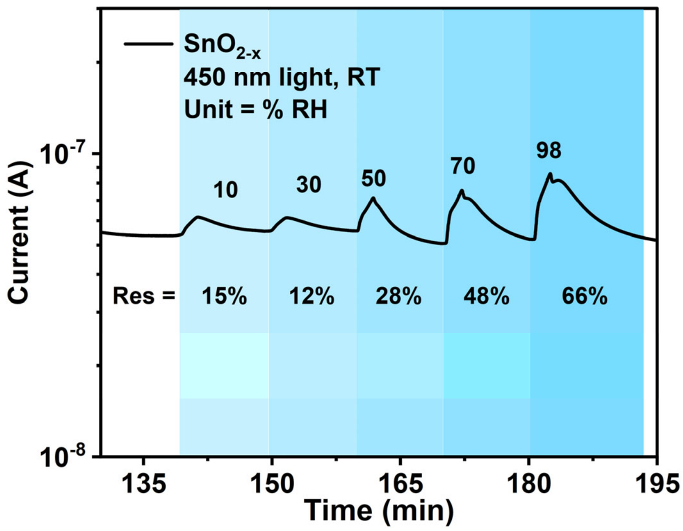


Fig. S13 Humidity sensing curve of $SnO_{2-x}$.

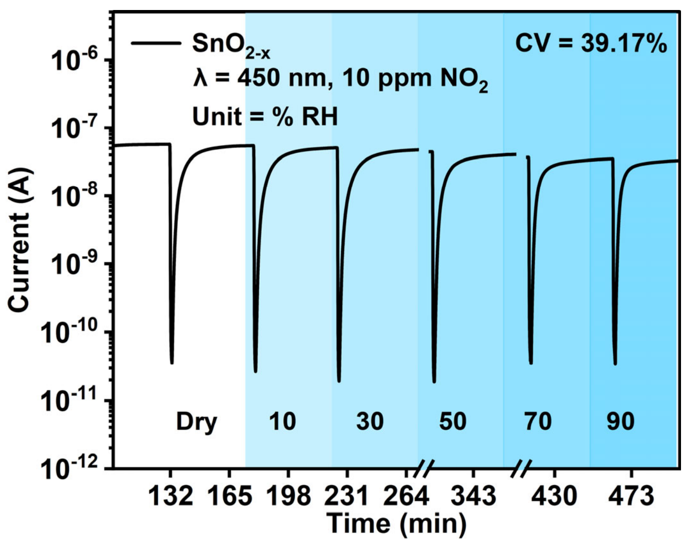


Fig. S14 Dynamic response curves of the $SnO_{2-x}$ sensor exposed to 10 ppm $NO_2$ under different relative humidity levels (Dry, 10%, 30%, 50%, 70%, and 90% RH) at room temperature under 450 nm light illumination.

**Table S1.** Room-temperature $NO_2$ sensing performance of different sensor devices under visible or UV light activation.

| Sensing materials | Light | LOD (ppb) | Res.%/Con. (ppm) | $t_{res}/t_{rec}$ (min) | Ref. |
|---|---|---|---|---|---|
| **$SnO_{2-x}$** | **Visible** | **0.006** | **2055300/100** | **0.5/120** | **This work** |
| HOF-1 | Vis. | 8 | 170000/100 | 2.5/0.6 | 1 |
| $SnO_2$/ZnO | UV | -- | 619/5 | 1.5/3.7 | 2 |
| ZnO | UV | -- | 410/20 | 3.7/2 | 3 |
| $TiO_2$@COF | Vis. | 1410 | 572/100 | 0.91/9.5 | 4 |
| Au/ZnO | Vis. | — | 60/5 | 25/ > 40 | 5 |
| Au-$SnO_2$ | Vis. | 6 | 17500/5 | 38.3/irr. | 6 |
| $Cu_3(HHTP)_2/Fe_2O_3$ | Vis. | 11 | 89/5 | ~ 30/120 | 7 |
| Zn-TDCOF-12 | Vis. | 7.9 | 54300/100 | 8.1/10.6 | 8 |
| ZnO/$SnO_2$ | UV | -- | $10^5$/0.5 | 7/8 | 9 |
| Pt-ZnO@PDA-1.5 nm | Vis. | 108 | 18489/100 | 0.37/- | 10 |
| $In_2O_3$ nanowire array | Vis. | 10 | 4.5/0.5 | 9/20 | 11 |
| 3D $TiO_2$ | Vis. | 0.2 | 370/5 | 7.1/16 | 12 |
| $TiO_2$@$NH_2$-MIL-125 | Vis. | 1.1 | 207/10 | 0.28/1.3 | 13 |
| ZnO | UV | -- | 120/20 | 15/48 | 14 |
| Cu/$Cu_2O$ | Vis. | -- | 527/10 | 0.5/-- | 15 |
| $SnO_2$@$SnS_2$ | Vis. | 1 | 520/0.2 | 15.8/19.3 | 16 |
| ZnO/g-$C_3N_4$ | Vis. | 38 | 4480/7 | 2.4/3.2 | 17 |
| $SnS_2$/rGO | Vis. | 5.03 | 650/1 | 1.3/4 | 18 |
| $SnS_2/TiO_2$ | Vis. | 1.7 | 40/1 | 0.72/1.7 | 19 |
| $SnS_2$ | Vis. | 38 | 1080/8 | 2.7/3.9 | 20 |
| $TiO_{2-x}N_x$ | UV-vis | -- | ~14/10 | ~6/6 | 21 |
| 2D $SnS_2$ | Vis. | 0.32 | 1430/5 | 12.2/62 | 22 |
| $ZnO_{1-x}$ | Vis. | -- | 259/1 | 13.7/15 | 23 |
| $NH_2$-terminated $SnO_2$ | UV-vis | -- | 2100/0.4 | 2.5/2.6 | 24 |
| $WO_3$ | Vis. | -- | 400/0.16 | 20/42 | 25 |
| GO@$TiO_2$ | UV-vis | 40 | 0.88/1 | 0.08/1.5 | 26 |
| CdS/ZnO | Vis. | 5 | 3.37/1 | 4E-4/4E-5 | 27 |
| 2D $SnS_2$ | Vis. | 0.464 | 11/0.05 | 7.7/-- | 28 |
| Au@$MoS_2$ | Vis. | 25 | ~27/10 | ~2/~2 | 29 |
| $In_2O_3$/Ru(II) | Vis. | -- | 175000/1 | --/-- | 30 |
| 3DOM ZIO | Vis. | 50 | 2160/0.05 | 1.9/2.1 | 31 |
| Au/$WS_2$ | Vis. | 13.6 | ~600/1 | ~1.2/-- | 32 |
| SV-$MoS_2$/ZnO | NIR | 0.1 | 226/0.2 | 1.25/1.85 | 33 |
| Black NiO | Vis. | 57 | 19.94/0.18 | 30/~70 | 34 |
| a-ZnO | Vis. | -- | 717/10 | 2 h/14 h | 35 |
| 2D $MoS_2$ | UV-vis | 1000 | 52.1/5 | 1.5/~1.7 | 36 |
| $SnO_2/MoS_2$ | Vis. | -- | 243/3 | ~5.5/~1.1 | 37 |
| $WO_3/CuWO_4$ | Vis. | 50 | 8100/1 | 1.55/0.47 | 38 |

| | | | | | |
|---|---|---|---|---|---|
| 0.5 wt% PTCDA/ZnO | Vis. | 7.4 | 10713/1 | 3.5/2.1 | [39] |
| Au/$SnS_2$ | Vis. | -- | 1100/1 | 11/9 | [40] |
| Au@$MoS_2$/SnS | Vis. | 25 | 450/1 | ~4/~4 | [41] |
| ZnO nanorods/Pd | Vis. | 0.2 | 160/0.1 | 0.4/0.5 | [42] |
| $In_2O_3$@ZnO | Vis. | -- | 180000/5 | 0.5/1.1 | [43] |
| MXene/$WS_2$ | Vis. | 100 | 60/10 | 0.93/0.88 | [44] |
| BiOI-ZnO | Vis. | 0.34 | ~370/0.1 | 0.3/0.17 | [45] |

"--" means cannot extracted the information from the article

# Reference


1 W.-H. Deng, L. He, E.-X. Chen, G.-E. Wang, X.-L. Ye, Z.-H. Fu, Q. Lin and G. Xu, *J. Mater. Chem. A*, 2022, **10**, 12977–12983.

2 N. Liu, H. Yu, Y. Yang and X.-T. Dong, *IEEE Sens. J.*, 2020, **20**, 2852–2859.

3 L. Meng, Q. Xu, Z. Sun, G. Li, S. Bai, Z. Wang and Y. Qin, *Mater. Lett.*, 2018, **212**, 296–298.

4 Y.-J. Chen, Y.-Y. Wen, W.-H. Li, Z.-H. Fu, G.-E. Wang and G. Xu, *Nano Lett.*, 2023, **23**, 3614–3622.

5 A. Gaiardo, B. Fabbri, A. Giberti, V. Guidi, P. Bellutti, C. Malagù, M. Valt, G. Pepponi, S. Gherardi, G. Zonta, A. Martucci, M. Sturaro and N. Landini, *Sens. Actuators, B*, 2016, **237**, 1085–1094.

6 K. Lim, Y.-M. Jo, J.-W. Yoon, J.-S. Kim, D.-J. Lee, Y. K. Moon, J. W. Yoon, J.-H. Kim, H. J. Choi and J.-H. Lee, *Small*, 2021, **17**, 2100438.

7 Y.-M. Jo, K. Lim, J. W. Yoon, Y. K. Jo, Y. K. Moon, H. W. Jang and J.-H. Lee, *ACS Cent. Sci.*, 2021, **7**, 1176–1182.

8 Y.-J. Chen, M. Liu, J. Chen, X. Huang, Q.-H. Li, X.-L. Ye, G.-E. Wang and G. Xu, *Chem. Sci.*, 2023, **14**, 4824–4831.

9 S. Park, S. An, Y. Mun and C. Lee, *ACS Appl. Mater. Interfaces*, 2013, **5**, 4285–4292.

10 Q. Liu, Y. Wen, J.-Z. Xiao, S.-Z. Luo, G.-E. Wang, P.-Y. Tang, X.-L. Ye and G. Xu, *Chin. J. Struct. Chem.*, 2023, **42**, 100069.

11 X.-X. Wang, H.-Y. Li and X. Guo, *J. Mater. Chem. A*, 2020, **8**, 14482–14490.

12 D. Cho, J. M. Suh, S.-H. Nam, S. Y. Park, M. Park, T. H. Lee, K. S. Choi, J. Lee, C. Ahn, H. W. Jang, Y.-S. Shim and S. Jeon, *Adv. Sci.*, 2021, **8**, 2001883.

13 W. Deng, M. Zhang, C. Li, M. Yao and G. Xu, *Angew. Chem., Int. Ed.*, 2024, e202419195.

14 S.-W. Fan, A. K. Srivastava and V. P. Dravid, *Sens. Actuators, B*, 2010, **144**, 159–163.

15 X. Zou, H. Fan, Y. Tian, M. Zhang and X. Yan, *Dalton Trans.*, 2015, **44**, 7811–7821.

16 D. Liu, Z. Tang and Z. Zhang, *Sens. Actuators, B*, 2020, **324**, 128754.

17 H. Wang, J. Bai, M. Dai, K. Liu, Y. Liu, L. Zhou, F. Liu, F. Liu, Y. Gao, X. Yan and L. Geyu, *Sens. Actuators, B*, 2020, **304**, 127287.

18 Y. Huang, W. Jiao, Z. Chu, G. Ding, M. Yan, X. Zhong and R. Wang, *J. Mater. Chem. C*, 2019, **7**, 8616–8625.

19 Q. Sun, Y. Li, J. Hao, S. Zheng, T. Zhang, T. Wang, R. Wu, H. Fang and Y. Wang, *ACS Appl. Mater. Interfaces*, 2021, **13**, 54152–54161.

20 D. Gu, X. Wang, W. Liu, X. Li, S. Lin, J. Wang, M. N. Rumyantseva, A. M. Gaskov and S. A. Akbar, *Sens. Actuators, B*, 2020, **305**, 127455.

21 W. I. Laminack and J. L. Gole, *Adv. Funct. Mater.*, 2013, **23**, 5916–5924.

22 T. H. Eom, S. H. Cho, J. M. Suh, T. Kim, T. H. Lee, S. E. Jun, J. W. Yang, J. Lee, S.-H. Hong and H. W. Jang, *J. Mater. Chem. A*, 2021, **9**, 11168–11178.

23 C. Zhang, X. Geng, H. Liao, C.-J. Li and M. Debliquy, *Sens. Actuators, B*, 2017, **242**, 102–111.

24 M. W. G. Hoffmann, J. D. Prades, L. Mayrhofer, F. Hernandez-Ramirez, T. T. Järvi, M. Moseler, A. Waag and H. Shen, *Adv. Funct. Mater.*, 2014, **24**, 595–602.

25 C. Zhang, A. Boudiba, P. De Marco, R. Snyders, M.-G. Olivier and M. Debliquy, *Sens. Actuators, B*, 2013, **181**, 395–401.

26 A. Berholts, M. Kodu, P. Rubin, T. Kahro, H. Alles and R. Jaaniso, *ACS Appl. Mater. Interfaces*,

2024, **16**, 43827–43837.
27 Z. Yang, L. Guo, B. Zu, Y. Guo, T. Xu and X. Dou, *Adv. Opt. Mater.*, 2014, **2**, 738–745.
28 K. Xu, N. Ha, Y. Hu, Q. Ma, W. Chen, X. Wen, R. Ou, V. Trinh, C. F. McConville, B. Y. Zhang, G. Ren and J. Z. Ou, *J. Hazard. Mater.*, 2022, **426**, 127813.
29 J. Hu, X. Liu, J. Zhang, X. Gu and Y. Zhang, *Sens. Actuators, B*, 2023, **382**, 133505.
30 A. Nasriddinov, S. Tokarev, O. Fedorova, I. Bozhev and M. Rumyantseva, *Chemosensors*, 2022, **10**, 135.
31 P. Yan, W. Hou, M. Wang, Y. Li, C. Ge, Z. Zhang, C. Tan, Y. Yin and L. Bai, *Sens. Actuators, B*, 2025, **426**, 137002.
32 Y. Sun, J. Hu and Y. Zhang, *Sens. Actuators, B*, 2022, **367**, 132032.
33 Y. Xia, C. Hu, S. Guo, L. Zhang, M. Wang, J. Peng, L. Xu and J. Wang, *ACS Appl. Nano Mater.*, 2020, **3**, 665–673.
34 X. Geng, D. Lahem, C. Zhang, C.-J. Li, M.-G. Olivier and M. Debliquy, *Ceram. Int.*, 2019, **45**, 4253–4261.
35 C. Zhang, J. Wang, M.-G. Olivier and M. Debliquy, *Sens. Actuators, B*, 2015, **209**, 69–77.
36 Y. Kang, S. Pyo, E. Jo and J. Kim, *Nanotechnology*, 2019, **30**, 355504.
37 Y. Kang, S. Pyo, D.-H. Baek and J. Kim, in *2017 19th International Conference on Solid-State Sensors, Actuators and Microsystems (TRANSDUCERS)*, IEEE, Kaohsiung, Taiwan, 2017, pp. 1429–1432.
38 Y. Liu, X. Li, X. Li, C. Shao, C. Han, J. Xin, D. Lu, L. Niu, Y. Tang and Y. Liu, *Sens. Actuators, B*, 2022, **365**, 131926.
39X. Cao, J. Hong, Z. Zhang, J. Li, J. Tang, J. Wang, D. Yi, X. Li, Y. Du and X. Tian, *Sens. Actuators, B*, 2023, **395**, 134464.
40 J. Hu, J. Zhang, X. Liu, H. Zhang, X.-X. Xue and Y. Zhang, *Appl. Surf. Sci.*, 2023, **623**, 157093.
41 J. Hu, Y. Zhao, B. Liu and Y. Zhang, *Sens. Actuators, B*, 2025, **433**, 137556.
42 J. Wang, C. Hu, Y. Xia and S. Komarneni, *Ceram. Int.*, 2020, **46**, 8462–8468.
43 Y. Li, X. Wei, Q. Liu, D. Zang and R. You, *ACS Sens.*, 2024, **9**, 3741–3753.
44 Y. Xia, S. He, J. Wang, L. Zhou, J. Wang and S. Komarneni, *Chem. Commun.*, 2021, **57**, 9136–9139.
45 Y. Li, Y. Liu, Y. Lu, Z. Liu, C. Sui, Y. Wang, L. Yang, F. Liu, P. Sun, F. Liu and G. Lu, *ACS Sens.*, 2022, **7**, 3915–3922.